TESTING THE NUMERICAL METHOD FOR ONE-DIMENSIONAL SHOCK TREATMENT

Andrej Horvat
Reactor Engineering Division
"Jožef Stefan" Institute
Ljubljana, Slovenia
E-mail: andrej.horvat@ijs.si

ABSTRACT - In the early 80's the SMUP computer code was developed at the "Jožef Stefan" Institute for simulation of two-phase flow in steam generators. It was suitable only for steady-state problems and was unable to simulate transient behaviour. In this paper, efforts are presented to find suitable numerical method to renew the old SMUP computer code. The obsolete numerical code has to be replaced with a more efficient one that would be able to treat time-dependent problems. It also has to ensure accurate solution during shock propagations. One-dimensional shock propagations in a tube were studied at zero viscosity. To simplify the equation of state the ideal gas was chosen as a working fluid. Stability margins in the form of transport matrix eigenvalues were calculated. Results were found to be close to those already published.

NOMENCLATURE

a	advection velocity
c	convection matrix term
CFL	Courant-Friedrichs-Levy criteria
d	diameter, pressure matrix term
f	friction factor
g	gravity acceleration
l	length
p	pressure
q	volumetric flow
R	gas constant
t	simulation time
T	temperature
u	momentum (ρv)
v	velocity
x	horizontal coordinate
z	vertical coordinate

Greek Letters

π	Ludolf's number
ρ	density
γ	numerical cell boundary
ω	numerical cell volume
Δ	finite difference

Subscripts / Superscripts

1	pressure calculation position
i	grid point index
$iMax$	max number of grid points
j	grid point index
n	number of iteration

INTRODUCTION

In the early 80's the SMUP computer code was developed at the "Jožef Stefan" Institute for simulation of two-phase flow in steam generators, which is extensively described in Gregorič et al. (1984) and in Petelin et al. (1986). The code was written as an incompressible flow code to calculate steady-state heat transfer and fluid flow behaviour. The code was unable to simulate transients and had very serious stability problems. Because of these deficiencies the code applicability was very limited.

In this paper efforts to find suitable numerical method to renew the old SMUP computer code are presented. The obsolete numerical code has to be replaced with a more efficient one which would be able to treat time-dependent problems. It also has to ensure an accurate solution during shock propagations. To determine the most suitable numerical scheme the accuracy and stability of different schemes were tested. Extensive testing revealed the numerical scheme which combines accuracy and also stability even at large time steps.

MODEL

The stability and accuracy of numerical schemes were tested using severe shock simulations in a pipe. The length of the pipe was *10m* and the shocks were always initiated at one half of its length. The pipe diameter was *0.1m*. Because of extensive experimental and computational work already done by others (Hirsch, 1990) the air was chosen as a working fluid. To further simplify the equation of state, the working fluid was considered an isothermal ideal gas. With the gas constant *287J/kgK* the initial pressure was *1bar* and the initial density *1.0kg/m*^{3}.

In many cases not only the Navier-Stokes equation but also the convection equation (eq. 1) and the Burger equation (eq. 2) are used to simulate transport phenomena in fluids.

$$\frac{\partial}{\partial t}(v) + a\frac{\partial}{\partial x}(v) = 0 \quad . \tag{1}$$

For testing convection equation (eq. 1) numerical scheme one-dimensional velocity shock propagations were studied. On the left side of the simulation domain the velocity was *300m/s* whereas on the other side the velocity was zero. At the inlet (e.g. on the left boundary) the Neumann boundary conditions were prescribed and at the outlet (e.g. on the right boundary) the second order boundary conditions were prescribed.

$$\frac{\partial}{\partial t}(v) + v\frac{\partial}{\partial x}(v) = 0 \quad . \tag{2}$$

Also, for testing the Burger equation (eq. 2) numerical scheme one-dimensional velocity shock propagations were studied. On the left side of simulation domain the velocity was *300m/s* whereas on the other side the velocity was zero. The boundary conditions at the inlet and outlet side where the same as in the case of convection equation (eq. 1).

$$\frac{\partial}{\partial t}(\rho v) + \frac{\partial}{\partial x}(v\,\rho v) = -\frac{\partial}{\partial x}(p) \quad . \tag{3}$$

For testing the Navier-Stokes equation (eq. 3) numerical scheme one-dimensional pressure shock propagations in a tube were used at zero viscosity. On the left side of the simulation domain the pressure was *1bar* whereas on the other side the pressure was *0.1bar*. Because the fluid flow also has to obey mass conservation law, the Navier-Stokes equation is coupled with the continuity equation:

$$\frac{\partial}{\partial t}(\rho) + \frac{\partial}{\partial x}(v\,\rho) = 0 \quad . \tag{4}$$

Basic criterion for boundary conditions was the mass conservation. At the left boundary second order boundary conditions for velocity and the Neumann boundary conditions for pressure were prescribed. At the outlet the Neumann boundary conditions for velocity and the second order boundary conditions for pressure were prescribed.

NUMERICAL METHODS

In all simulated cases the numerical mesh had 101 grid points (fig. 1). The time and space discretisations were first order accurate. For all three cases the finite volume method (Versteeg & Malalasekera, 1995) was applied with the upwind discretisation of the fluxes.

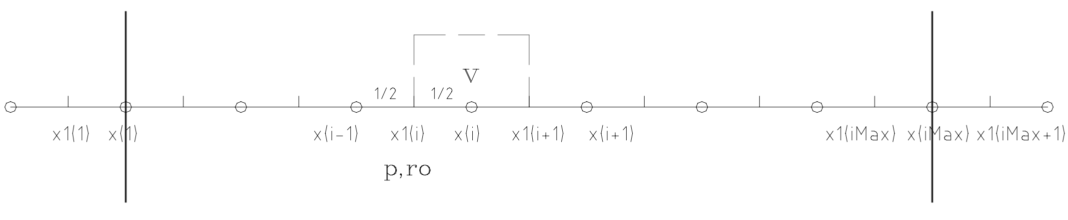

Fig. 1: Numerical mesh arrangement.

For time integration of the convection equation the explicit Euler method was used. In matrix form the convection equation (eq. 1) is written as:

$$v_{x(j)}^{n+1} = \left(a^{+} \frac{\Delta t}{\omega_{x(j)}} \gamma_{x1(j)} \right) v_{x(j-1)}^{n} + \left(1 + \frac{\Delta t}{\omega_{x(j)}} \left(a^{-} \gamma_{x1(j)} - a^{+} \gamma_{x1(j+1)} \right) \right) v_{x(j)}^{n} + \left(-a^{-} \frac{\Delta t}{\omega_{x(j)}} \gamma_{x1(j+1)}^{n} \right) v_{x(j+1)}^{n} \tag{5}$$

where the advection velocities are defined as:

$$a^{+} = \frac{1\cdot}{2}\left(a + |a| \right) \text{ and } a^{-} = \frac{1\cdot}{2}\left(a - |a| \right). \tag{6}$$

Also, for time integration of the Burger equation the explicit Euler method was used. In matrix form the Burger equation (eq. 2) is written as:

$$v_{x(j)}^{n+1} = \left(a_{x1(j)}^{+} \frac{\Delta t}{\omega_{x(j)}} \gamma_{x1(j)} \right) v_{x(j-1)}^{n} + \left(1 + \frac{\Delta t}{\omega_{x(j)}} \left(a_{x1(j)}^{-} \gamma_{x1(j)} - a_{x1(j+1)}^{+} \gamma_{x1(j+1)} \right) \right) v_{x(j)}^{n} + \left(-a_{x1(j+1)}^{-} \frac{\Delta t}{\omega_{x(j)}} \gamma_{x1(j+1)}^{n} \right) v_{x(j+1)}^{n} \tag{7}$$

where the advection velocities are defined as

$$\begin{aligned} a_{x1(j+1)}^{+} &= \frac{1}{4}\left(\left(v_{x(j)} + v_{x(j+1)} \right) + \left| v_{x(j)} + v_{x(j+1)} \right| \right) , \\ a_{x1(j+1)}^{-} &= \frac{1}{4}\left(\left(v_{x(j)} + v_{x(j+1)} \right) - \left| v_{x(j)} + v_{x(j+1)} \right| \right) , \\ a_{x1(j)}^{+} &= \frac{1}{4}\left(\left(v_{x(j-1)} + v_{x(j)} \right) + \left| v_{x(j-1)} + v_{x(j)} \right| \right) , \\ a_{x1(j)}^{-} &= \frac{1}{4}\left(\left(v_{x(j-1)} + v_{x(j)} \right) - \left| v_{x(j-1)} + v_{x(j)} \right| \right) . \end{aligned} \tag{8}$$

They are functions of calculated velocities and they are not constant as in the case of the convection equation (eq. 5).

In the Navier-Stokes equation, the pressure is also introduced as one of the simulated variables. Although only the staggered grid arrangement for pressure field (fig. 1) is presented here, the collocated grid arrangement (Ferziger & Perić, 1996) was also extensively tested. A stable numerical algorithm however, was not found. For time integration of Navier-Stokes equation the projection method was used (Bell et al., 1989), where the time integration is split into separate stages:

$$(\rho v)^{n+1/2} = (\rho v)^{n} - \Delta t \frac{\partial}{\partial x} (v \cdot \rho v)^{n} , \tag{9}$$

$$(\rho v)^{n+1} = (\rho v)^{n+1/2} - \Delta t \frac{\partial}{\partial x} (p)^{n+1} . \tag{10}$$

The convection part was integrated explicitly with the Euler method and the continuity equation was treated implicitly:

$$\rho^{n+1} + \Delta t \frac{\partial}{\partial x} (\rho v)^{n+1} = \rho^{n} . \tag{11}$$

In matrix form (eq. 9) is written as:

$$u_{x(j)}^{n+1/2} = \left(a_{x1(j)}^{+} \frac{\Delta t}{\omega_{x(j)}} \gamma_{x1(j)} \right) u_{x(j-1)}^{n} + \left(1 + \frac{\Delta t}{\omega_{x(j)}} \left(a_{x1(j)}^{-} \gamma_{x1(j)} - a_{x1(j+1)}^{+} \gamma_{x1(j+1)} \right) \right) u_{x(j)}^{n} + \left(-a_{x1(j+1)}^{-} \frac{\Delta t}{\omega_{x(j)}} \gamma_{x1(j+1)}^{n} \right) u_{x(j+1)}^{n} \tag{12}$$

where the advection velocities are defined as in the case of the Burger equation (eq. 7). The first stage of the Navier-Stokes equation (eq. 9) is then combined with the continuity equation (eq. 11) into the pressure equation (eq. 13) to satisfy mass conservation at time level *n+1*.

$$\frac{p^{n+1}}{RT} - \Delta t^2 \frac{\partial^2}{\partial x^2}\left(p^{n+1}\right) = \frac{p^n}{RT} - \Delta t \frac{\partial}{\partial x}(\rho v)^{n+1/2} . \tag{13}$$

The pressure equation (eq. 13) in matrix form is then written as:

$$\left(-\gamma_{x1(j-1)}\Delta t \frac{\gamma_{x(j-1)}}{\omega_{x(j-1)}}\right)p^{n+1}_{x1(j-1)} + \left(\frac{\omega_{x1(j)}}{dt\,RT} + \gamma_{x1(j)}\Delta t\left(\frac{\gamma_{x(j-1)}}{\omega_{x(j-1)}} + \frac{\gamma_{x(j)}}{\omega_{x(j)}}\right)\right)p^{n+1}_{x1(j)} + \left(-\gamma_{x1(j+1)}\Delta t \frac{\gamma_{x(j)}}{\omega_{x(j)}}\right)p^{n+1}_{x1(j+1)} = \tag{14}$$

$$= p^n_{x1(j)} \frac{\omega_{x1(j)}}{\Delta t\, RT} - \left(u^{n+1/2}_{x(j)}\gamma_{x(j)} - u^{n+1/2}_{x(j-1)}\gamma_{x(j-1)}\right) \quad .$$

After pressure calculation, which was in this case done with the Gauss-Jordan elimination (Press et al., 1993), the velocity is updated with pressure gradient:

$$u^{n+1}_{x(j)} = u^{n+1/2}_{x(j)} - \frac{\Delta t}{\omega_{x(j)}}\left(p^{n+1}_{x1(j+1)}\gamma_{x1(j+1)} - p^{n+1}_{x1(j)}\gamma_{x1(j)}\right) \quad . \tag{15}$$

STABILITY

The stability of numerical schemes for convection dominated problems was usually connected with Courant-Friedrichs-Levy condition:

$$CFL = \frac{v\Delta x}{\Delta t} \quad , \tag{16}$$

where v is the advection velocity. For pure convection equation (eq. 1) and most of the numerical schemes the CFL condition is easy to calculate (e.g. CFL condition for upwind discretisation is $0 < CFL \leq 1$). This approach does not take into account the influence of boundary conditions and also fails when it is applied to non-linear problems such as the Burger equation (eq. 2) or the Navier-Stokes equation (eq. 3).

Another approach to stability analysis is the so-called matrix method (Hindmarsh et al., 1984), which also takes into account the boundary conditions (vector S) :

$$\frac{\Delta\vec{v}}{\Delta t} = \underline{A}\vec{v} + \vec{S} . \tag{17}$$

The solution of (eq. 17) stays stable when the real part of matrix A eigenvalues is bounded:

$$\left|\mathrm{Re}(\lambda)\right| \leq 1 . \tag{18}$$

When the matrix method stability criteria (eq. 18) is applied to the Euler scheme with upwind discretisation, the calculated stable range is twice as wide as before. This was however not proved in practice and was strongly criticised (Hindmarsh et al., 1984).

To avoid this misunderstanding of matrix method stability conditions, a more general matrix analysis was applied. This method can be also used for linear and non-linear convection problem in one, two or three dimensions. In general, the (eq. 5, 7, 12) can be written in matrix form as:

$$\vec{v}^{\,n+1} = \underline{C} \cdot \vec{v}^{\,n} . \tag{19}$$

The vector v at $n+1$ is calculated when vector v at n is multiplied with the transport matrix C:

$$\underline{C} = \sum_{j=1}^{n} \lambda_j \vec{e}_j \otimes \vec{e}_j . \tag{20}$$

Each vector v can be also decomposed into the eigenvectors e of operator C :

$$\vec{v}^{\,n} = \sum_{j=1}^{n} \xi_j \vec{e}_j . \tag{21}$$

When the vector v is repeatedly multiplied with operator C as in the case of numerical simulation, the stability of the numerical scheme depends only on operator C eigenvalues:

$$\underline{C} \cdot \vec{v} = \sum_{j=1}^{n} \lambda_j \vec{v}_j \ . \tag{22}$$

To ensure stable numerical iterations the eigenvalues have to be not only bounded but also the real part of each eigenvalue has to be larger than 0:

$$stable = \begin{cases} |\lambda| \ \le \ 1 \\ \mathrm{Re}(\lambda) > 0 \end{cases} . \tag{23}$$

For the eigenvalues calculation the asymmetric matrices C were first balanced and then transformed into Hessenberg form. Next, the QR decomposition was used to obtain complex eigenvalues. The mathematical and numerical procedures are well described in Golub & Van Loan (1996).

RESULTS

Numerical simulations of shock propagations were performed using the convection equation, the Burger equation and the Navier-Stokes equation. In all cases the same numerical grid and simulation time interval *0.008s* were applied. Only the number of time iterations and the timestep were changed from case to case to show the stability eigenvalues dependence. The simulations also revealed that in all cases eigenvalues stay real during time iterations.

For the convection equation numerical simulations with *100*, *50*, *25* and *23* time iterations were done. These corresponds to timesteps of *0.00008s*, *0.00016s*, *0.0032s*, *0.00348s* and to the *CFL* values of *0.24*, *0.48*, *0.96*, *1.043*, respectively. Because of the clarity only the examples with *50* and *23* time iterations are presented.

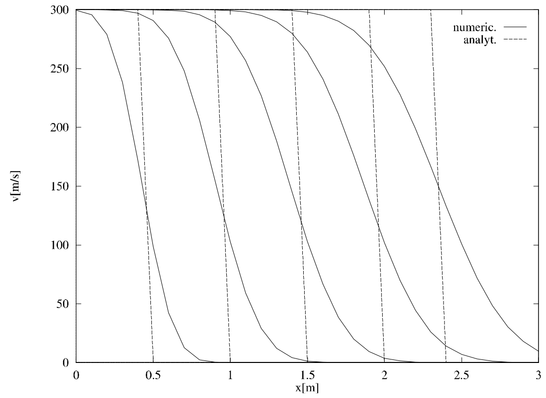

Fig 2. Shock propagation (50 iterations).

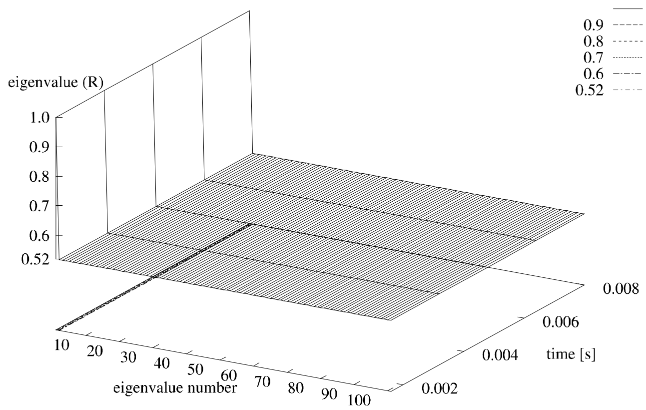

Fig 3. Eigenvalues time distribution (50 iterations).

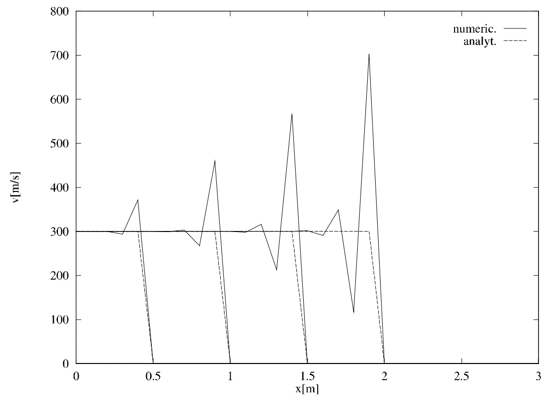

Fig 4. Shock propagation (23 iterations).

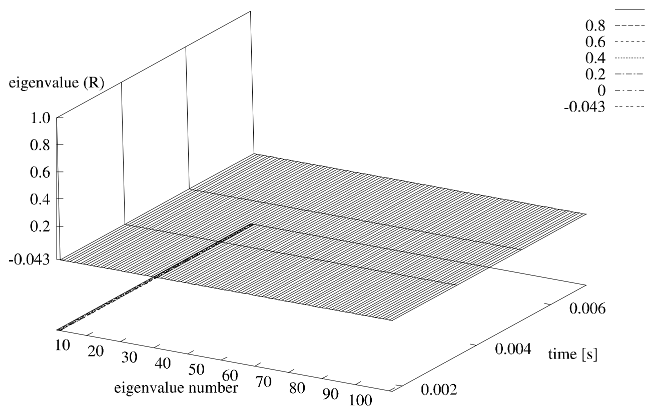

Fig 5. Eigenvalues time distribution (23 iterations).

It can be observed on fig. 2 and 4 that the instability of numerical scheme is increased when the number of time iterations is reduced or when the timestep is enlarged. On fig. 3 and 5 the time developments of the transport matrix eigenvalues are presented. Because the advection velocity *a* is constant, the eigenvalues stays unchanged during the entire time integration. The largest eigenvalue on the left is one due to predefined velocity at the inlet boundary. As the number of time iterations is reduced (from *50* to *23*) and the timestep is increased (from *0.00016s* to *0.00348s*) the *n-1* eigenvalues are approaching zero, which clearly indicates unstable behaviour (fig. 5).

For the Burger equation numerical simulations with *200*, *100* and *51* time iterations were carried out. This corresponds to timesteps of *0.00004s*, *0.00008s*, *0.000157s* and to the *CFL* values of *0.12*, *0.24*, *0.471*, respectively. Because of the clarity only the examples with *200* and *51* time iterations are presented.

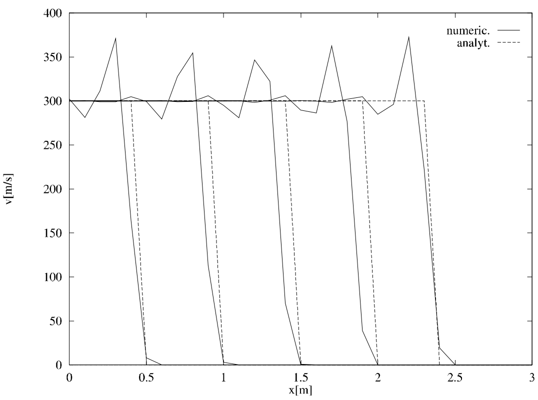

Fig 6. Shock propagation (200 iterations).

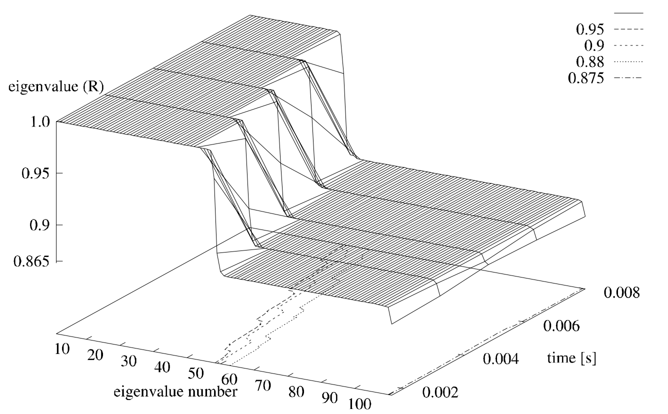

Fig 7. Eigenvalues time distribution (200 iterations).

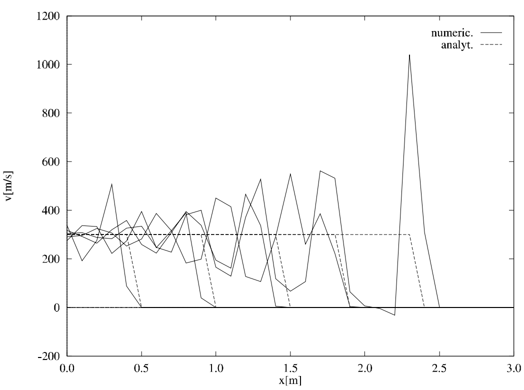

Fig 8. Shock propagation (51 iterations).

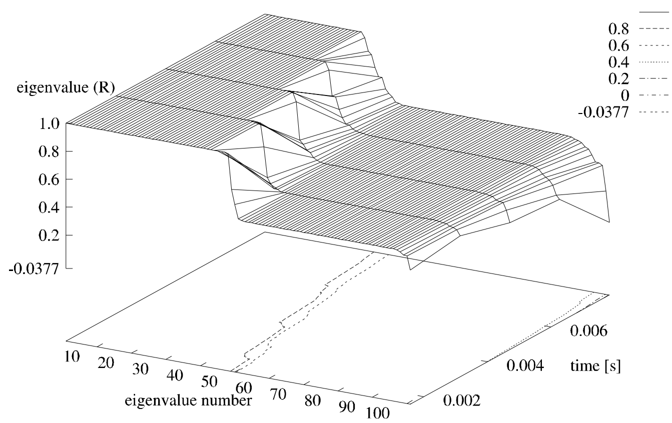

Fig 9. Eigenvalues time distribution (51 iterations).

Again the examples on fig. 6 and 8 show the increased instabilities when the number of time iterations is reduced or when the timestep is enlarged. This is the case where the *CFL* condition fails to predict unstable behaviour. The *CFL* condition is *0.471* when numerical integration already diverges. On the other hand, the time developments of the transport matrix eigenvalues on the fig. 7 and 9 clearly show when one of the eigenvalues is approaching zero. This results in growing instabilities.

In the case of the Navier-Stokes equation the developed numerical code was first verified by comparing calculated and analytically obtained results of pressure shock propagation in Tiselj (1997).

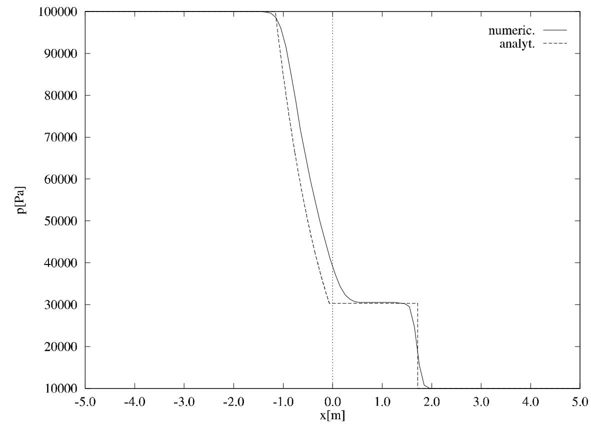

Fig 10. Pressure comparison (*t = 0.0031s*).

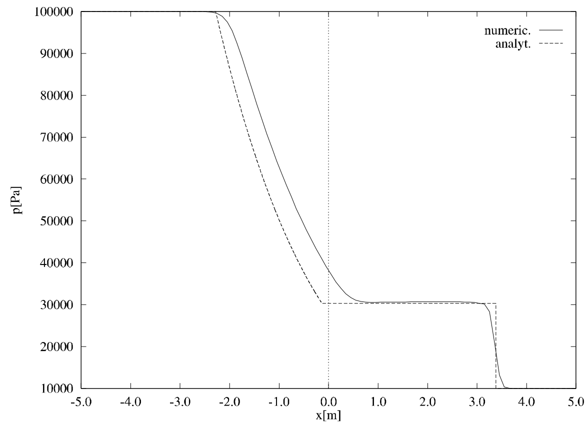

Fig 11. Pressure comparison (*t = 0.0061s*).

As presented on fig. 10 and 11, the numerically calculated results are close to those already published, which justifies the described approach for compressible flow treatment. The numerically calculated density and velocity field differ from the analytically calculated for about 20 percent due to isothermal ideal gas approximation of the working fluid.

The numerical simulation of pressure shock propagations were performed with *200*, *100, 50* and *45* time iterations. These correspond to timesteps of *0.00004s*, *0.00008s*, *0.00016s, 0.000178s* and to the *CFL* values of *0.12*, *0.24*, *0.48*, *0.53*, respectively. Because of the clarity only the examples with *200* and *45* time iterations are presented.

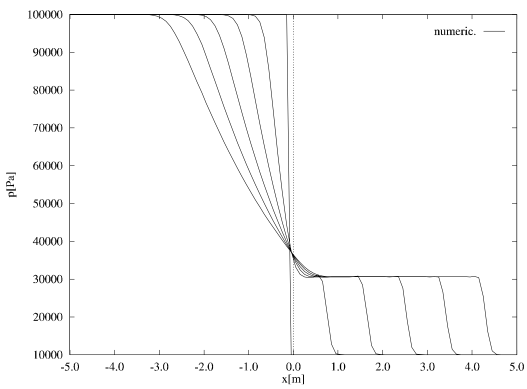

Fig 12. Shock propagation (200 iterations)

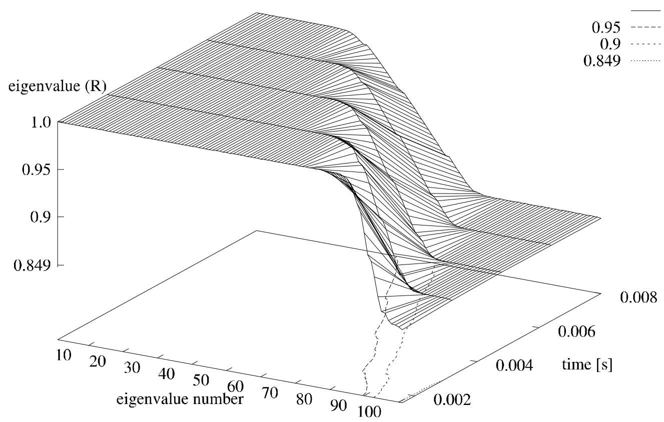

Fig 13. Eigenvalues time distribution (200 iterations).

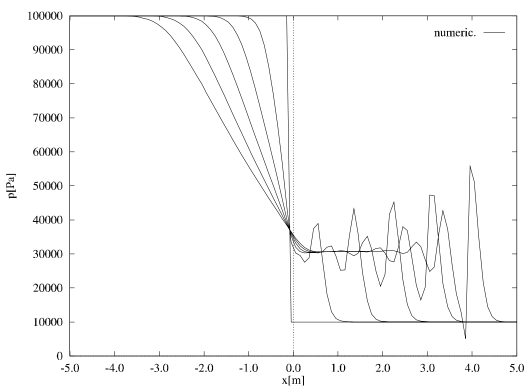

Fig 14. Shock propagation (45 iterations)

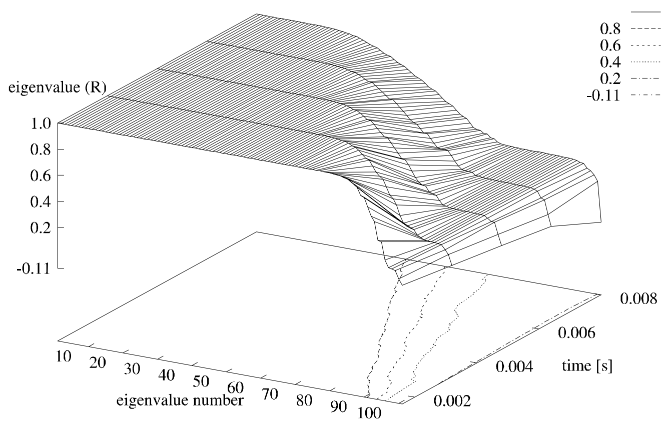

Fig 15. Eigenvalues time distribution (45 iterations).

Again, the examples on fig. 12 and 14 show the increased instabilities when the number of time iterations is reduced or when the timestep is enlarged. The stability analysis of Navier-Stokes equation is more complicated because of the pressure field that forces the mass conservation. In spite of fact that a complete stability analysis of the Navier-Stokes equation should also include pressure, the instabilities are principally governed by the size of the transport matrix eigenvalues. As fig. 13 and 15 show, the instabilities occur immediately when one of the eigenvalues becomes negative.

CONCLUSIONS

The stability of first order accurate schemes for convection problems were analysed in order to find a suitable numerical algorithm for the old SMUP code. For this purpose velocity shocks were simulated using the convection equation and the Burger equation. The compressible form of Navier-Stokes equation was applied for pressure shock testing. Results of code verification justify the selected numerical algorithm.

For stability analysis the matrix method was modified and the new stability criteria were developed. These criteria are based on calculated eigenvalues of the so-called transport matrix. Results of eigenvalue computations during simulations, when the convection equation or the Burger equation was applied, prove the accuracy of the introduced stability criteria. The same criteria were also applied to the Navier-Stokes equation during pressure shock calculation. Although the eigenvalues calculation of the convection part of the Navier-Stokes equation is inadequate as precise stability criteria, the simulations showed that instabilities are principally governed by the size of eigenvalues.

In the future the stability of the Navier-Stokes equation will be further investigated to clarify the stability conditions and ensure a solid base for time dependent flow modelling.

REFERENCES

Bell, J. B., Colella, P., Glaz, H. M., 1989, "A Second Order Projection Method for the Incompressible Navier-Stokes Equation", J. Comp. Phys. , 2, 1989, pp. 257-283.

Ferziger, J. H., Periæ, M., 1996, "Computational Method for Fluid Dynamics", Springer Verlag, Berlin, pp. 184-188.

Golub, G. H., Van Loan, C. F., 1996, "Matrix Computations", 3rd Edition, John Hopkins, Baltimore, pp. 308-391.

Gregorič, M., Peterlin, G., Petelin, S., Mavko, B., Radović, M., Željko, M., 1984, "Spremljanje problematike uparjalnikov", IJS-DP-3501, Ljubljana.

Hindmarsh, A. C., Gresho, P. M., Griffits, D. F., 1984, "The Stability of Explicit Euler Time-Integration for Certain Finite Difference Approximations of the Multi-Dimensional Advection-Diffusion Equations", Int. J. Num. Meth. in Fluids, 1984, Vol. 4, pp. 853-897.

Hirsch, C., 1990, "Numerical Computation of Internal and External Flows", John Willey & Sons, Chichester.

Petelin, S., Mavko, B., Gregorič, M., Kostadinov, V., 1986, "Toplotna in hidravlična analiza razmer v uparjalniku z upoštevanjem čepljenja", IJS-DP-4374, Ljubljana,.

Press, W. P., Flannery, B. P., Teukolsky, S. A., Vetterling, W. T., 1993, "Numerical Recipes in C", Cambridge Press, Cambridge, pp. 36-41.

Tiselj, I., 1997, "Second Order Accurate Schemes for Two-Fluid Models of Two-Phase Flow", Ph.D. Thesis, Ljubljana, p. 52.

Versteeg, H. K., Malalasekera, W., 1995, "An Introduction to Computational Fluid Dynamics, The Finite Volume Method", Longman Scientific & Technical, England, pp. 103-133 .